Journal of Neurochemistry, 2004, **89**, 1241–1251 doi:10.1111/j.1471-4159.2004.02428.x

A low molecular weight copper chelator crosses the blood–brain barrier and attenuates experimental autoimmune encephalomyelitis

Daniel Offen,* Yossi Gilgun-Sherki,* Yael Barhum,* Moran Benhar,† Leonid Grinberg,† Reuven Reich,‡ Eldad Melamed* and Daphne Atlas†

*Neurology Department and Felsenstein Medical Research Center Tel Aviv University, Rabin Medical Center, Petah-Tikva, Israel
†Department of Biological Chemistry, Institute of Life Sciences, The Hebrew University of Jerusalem, Jerusalem, Israel
‡Department of Pharmacology, School of Pharmacy and David R. Bloom Center for Pharmacy, The Hebrew University, Jerusalem, Israel

Abstract

Increasing evidence suggests that enhanced production of reactive oxygen species (ROS) activates the MAP kinases, c-Jun N-terminal protein kinase (JNK) and mitogen-activated protein kinase MAPK (p38). These phosphorylated intermediates at the stress-activated pathway induce expression of matrix metalloproteinases (MMPs), leading to inflammatory responses and pathological damages involved in the etiology of multiple sclerosis (MS). Here we report that *N*-acetylcysteine amide (AD4) crosses the blood–brain barrier (BBB), chelates Cu^{2+}, which catalyzes free radical formation, and prevents ROS-induced activation of JNK, p38 and MMP-9. In the myelin oligodendrocyte glycoprotein (MOG)-induced experimental autoimmune encephalomyelitis (EAE), a mouse model of MS, oral administration of AD4 drastically reduced the clinical signs, inflammation, MMP-9 activity, and protected axons from demylination damages. In agreement with the *in vitro* studies, we propose that ROS scavenging by AD4 in MOG-treated animals prevented MMP's induction and subsequent damages through inhibition of MAPK pathway. The low toxicity of AD4 coupled with BBB penetration makes this compound an excellent potential candidate for the therapy of MS and other neurodegenerative disorders.

Keywords: AD4, blood–brain barrier, experimental autoimmune encephalomyelitis, multiple sclerosis, oxidative stress, reactive oxygen species, thiol-antioxidants.
J. Neurochem. (2004) **89,** 1241–1251.

Free radicals and other reactive oxygen species (ROS) constitute a normal part of the intracellular machinery milieu. Endogenously, enzymes such as catalase, superoxide dismutase, and the thiol redox systems GSH/GSSG (glutathione/oxidized glutathione) and thioredoxin serve as reducing agents to minimize the harm ROS might cause in the cell. An excess of ROS, however, can tilt the delicate balance leading to oxidative stress (OS). Indeed, OS appears to play an important role in the pathogenesis of progressive neurodegenerative disorders such as Alzheimer's disease, Parkinson's disease, amyotrophic lateral sclerosis (ALS), multiple sclerosis (MS) and acute syndromes of neurodegeneration, such as ischemic and hemorrhagic stroke (Rothstein 1996; Sen 1998; Butterfield *et al*. 1999; Finkel and Holbrook 2000; Gilgun-Sherki *et al*. 2002).

OS is heavily implicated in the inflammatory process characterized by overproduction of ROS ($\cdot O_2^-$, $\cdot OH$, H_2O_2) and reactive nitrogen species (RNS) (NO, ONOO-ROS/RNS). Copper, a redox-active metal, and zinc, which play important catalytic roles in many enzyme activities also catalyze free radical formation and drive OS. Chelation of copper/zinc was demonstrated to rapidly inhibit β-amyloid accumulation in Alzheimer's disease transgenic mice (Cherny *et al*. 2001) most likely preventing [Aβ–Cu] complexes that through Cu^{2+} reduction generate neurotoxic H_2O_2 (Opazo *et al*. 2002).

Received 12 November, 2003; revised manuscript received 27 January, 2004; accepted 29 January, 2004.

Address correspondence and reprint requests to Daphne Atlas, Department of Biological Chemistry, Institute of Life Sciences, The Hebrew University of Jerusalem, Campus Edmond Safra, Jerusalem, 91904, Israel. E-mail: datlas@vms.huji.ac.il

Abbreviations used: AD4, *N*-acetylcysteine amide; BBB, blood–brain barrier; BSO, buthionine sulfoximine; EAE, experimental autoimmune encephalomyelitis; GSH, glutathione; HTA, hydroxyterphthalic; JNK, c-Jun N-terminal protein kinase; MMP, matrix metalloproteinase; MOG, myelin oligodendrocyte glycoprotein; MS, multiple sclerosis; NEM, *N*-ethylmaleimide; OS, oxidative stress; PBS, phosphate-buffered saline; ROS, reactive oxygen species.

The induction of neutrophils, lymphocytes, and macrophages, which release ROS, RNS, and lytic enzymes, amplify the inflammatory reaction (Yong *et al*. 2001). OS activates gene expression of pro-inflammatory cytokines, such as interleukin-1β,4 and interleukin-6,5.

The concept now emerging is that ROS specifically target components of mitogen-activated protein kinase (MAPK) pathways. The MAPKs constitute a large family of proline-directed, serine/threonine kinases activated by upstream dual-specific MAPK kinases (MAPKKs), which themselves are activated by MAPKK kinases (Boulton *et al*. 1991; Davis 1993; Takahashi and Berk 1998; Adler *et al*. 1999). In turn, MAPKs phosphorylate selected intracellular proteins including transcription factors, e.g. c-Jun, MTF2, ERK subsequently regulating gene expression, cellular proliferation, inflammation, and apoptosis. Therefore, free radical scavenging is predicted to block activation of MAPK-pathway proteins preventing the phosphorylation of c-Jun N-terminal protein kinase (JNK) and p38 mitogen-activated protein (Davis 1993).

A strong link between OS and MS has been suggested. In the mouse model of experimental autoimmune encephalomyelitis (EAE), several studies have shown protective effects and suppression of EAE by antioxidants (Lehmann *et al*. 1994; Marracci *et al*. 2002).

One of the powerful endogenous defensive mechanisms against free radicals in many diseases is the heme oxygenase-1 (HO-1) that is induced by OS (Emerson and LeVine 2000). In MS it was demonstrated that interferon-β attenuated glial HO-1 gene induction (Liu *et al*. 2001; Mehindate *et al*. 2001). Moreover, metalloproteinases (MMPs) are activated during the inflammation process and high MMP-9 levels were detected in the cerebrospinal fluid of MS patients and other inflammatory neurologic diseases but not in normal control patients (Gijbels *et al*. 1992; Cuzner *et al*. 1996; Lindberg *et al*. 2001).

In the past decade, a multitude of natural reducing agents such as vitamin E, carotenoids, flavonoids, lipoic acid, the synthetic lazaroid (tirilazad) and *N*-acetyl cysteine have been used as protectors against OS (Sen 1998; Gilgun-Sherki *et al*. 2001; Gilgun-Sherki *et al*. 2002). Even though clinical evidence have demonstrated that such compounds act as protective drugs in neurodegenerative diseases, their use is still relatively limited mainly due to the inability of some, to cross the blood–brain barrier (BBB) or getting pass the cell membrane.

In the present study, we characterize the chemical and redox properties of *N*-acetylcysteine amide (AD4), a low molecular weight thiol-compound (Atlas *et al*. 1999) that, unlike *N*-acetyl cysteine, readily crosses the BBB. We show that AD4 scavenges ROS, inhibits phosphorylation of MAPKs (p38 mitogen-activating protein and JNK) and MMPs' activation. *In vivo*, using a mouse model of MS, AD4 drastically reduced clinical signs, inflammation and MMP-9 production. We therefore suggest that MAPK signaling in MS could be a target for inhibiting pathogenic consequences of elevated ROS. Therefore, AD4 could become a potential candidate for treating MS and other neurodegenerative diseases.

Materials and methods

Reagents

Reagents used were as follows: anti-JNK1, anti-p38 (Santa Cruz Biotechnology, Santa Cruz, CA, USA); anti-phospho-p38, anti-phospho-JNK (Cell Signaling Technology, Beverly, MA, USA); SMI-32 (Sternberger Monoclonals, Baltimore, MD, USA); Cy™ 3-conjugated donkey anti-mouse IgG (Jackson Immunoresearch Laboratory West Grove, PA, USA); cisplatin (CDDP; ABIC, Netanya, Israel); dichlorofluorescein bis(acetoxymethyl) diacetate (Molecular Probes, Eugene, OR, USA); and myelin oligodendrocyte glycoprotein (MOG; Weizmann Institute, Rehovot, Israel). Other chemicals were purchased from Sigma (St Louis, MO, USA).

Copper chelation

Hydroxyl radicals (·OH) were generated in the presence of ascorbic acid (Asc-H_2) with air oxygen and copper ions. Terephthalic acid (TA), capable of scavenging ·OH and thereby converting into fluorescent hydroxyterphthalic acid (HTA) (Barreto *et al*. 1995) was used to monitor ·OH levelS:

$$\text{Asc-H}_2 + 2\text{Cu}^{2+} \rightarrow \text{Asc} + 2\text{Cu}^{+} + 2\text{H}^{+} \quad (1)$$

$$\text{Cu}^{+} + \text{H}^{+} + \text{O}_2 \rightarrow \text{Cu}^{2+} + \text{H}_2\text{O}_2 \quad (2)$$

$$\text{H}_2\text{O}_2 + \text{Cu}^{+} \rightarrow \cdot\text{OH} + \text{OH}^{-} + \text{Cu}^{2+} \quad (3)$$

$$\text{TA} + \cdot\text{OH} \rightarrow \text{HTA(fluorescent)} \quad (4)$$

The reaction mixture of 5 mM TA, 20 μM $CuSO_4$, 1 mMAsc-H_2, 10 mM Na-phosphate buffer, pH 7.4 and AD4 was at the indicated concentrations. The reaction was initiated by ascorbate and 30-s aliquots were assayed for HTA fluorescence at 315/425 nm (excitation/emission).

Thiol content of RBC

RBC were obtained from fresh human blood washed twice and re-suspended in equal volume of phosphate-buffered saline (PBS). RBC thiols were depleted by applying tert-butylhydroxyperoxide (t-BHP) at 37°C. The reaction was cooled, washed twice, re-suspended in PBS and the tested reagents were co-incubated for 30–120 min at 37°C. Thiol determination was according to the modified procedure of Beutler (1974). In normal RBC, ~98% of thiols is GSH. Methemoglobin (MetHb) content was determined according to Grinberg *et al*. (1994).

Cell culture and treatment

EGF-transformed NIH3T3 cells (DHER14 cells) have been described (Benhar *et al*. 2001). Human neuroblastoma SHSY5Y cells were maintained in Dulbecco's modified Eagle's medium, and in protection experiments cells (100 μL of 3×10^5 cells/mL) were subcultured in 2% fetal calf serum plated on poly L-lysine-coated microtiter plates.

Immunoblotting

Cells were lysed (20 mM Tris, pH 7.5, 250 mM NaCl, 0.5% NP-40, 3 mM EDTA, 3 mM EGTA, 10% glycerol, 20 mM β-glycerolphosphate, 1 mM of *p*-nitrophenyl phosphate, 0.5 mM Na_3VO_4, 1 mM dithiothreitol, 2 μg/mL leupeptin, 2 μg/mL aprotonin and 1 mM AEBSF, and centrifuged (20 000 × *g*, 15 min, 4°C). Protein lysate (30 μg) (modified Bradford method; Zor and Selinger 1996) separated by sodium dodecyl sulfate–polyacrylamide gel electrophoresis, blotted, exposed to selective antibodies and visualized by enhanced chemiluminescence. Densitometry of immunoblots performed with NIH image 1.61.

Determination of ROS

Production of ROS was detected by fluorometric DCF assay, using dichlorofluorescein diacetate bis(acetoxymethyl) (DCF-DA). Cells loaded with 10 μM of DCFH-DA in serum-free medium (30 min, 37°), washed, and incubated in phenol red-free medium. Fluorescence was monitored at 485/538 nm in microplate fluorimeter (FLUOstar).

Animals

Six to 8-week-old C3H.SW/C57/bL female mice weighing 20 g were obtained from Harlan Laboratories, Rehovot, Israel. The animals were housed in standard conditions: constant temperature (22 ± 1°C), humidity (relative, 30%) and a 12-h light/dark cycle, and were allowed free access to food and water. The animals and protocol procedures were approved and supervised by the Animal Care Committee at the Rabin Medical Center.

Induction of chronic EAE

Chronic EAE was induced according to previous procedures (Whitham *et al*. 1991). Briefly, female C3H.SW or C57/bL mice (6–8 weeks old) were immunized twice, at day 1 and day 8, by subcutaneous injection with an emulsion containing myelin oligodendrocyte glycoproteins (pMOG35-55 × 3.75 mg/kg in C3H.SW and 15 mg/kg in C57/bL) and incomplete Freund's adjuvant (CFA), 200 μg heat-activated *Mycobacterium tuberculosis* in a total volume of 0,2 mL. AD4 was administrated intraperitoneally from day one (first MOG injection) or day 8. The first symptom appeared with a mean ± SE, $n = 10$–15. A large number of animals developed acute EAE clinical signs 14–18 days after immunization. Mice were scored for clinical signs using a score scale: 0, no paralysis; 1, loss of tail tonicity; 2, mild hind limb weakness; 3, complete hind limb paralysis; 4, paralysis of four limbs; 5, total paralysis; 6, death (Mendel *et al*. 1998).

Histopathology

Whole spinal colons from six control MOG- and six MOG + AD4-treated mice were dissected 30 days after immunization with the MOG peptide (pMOG 35–55), fixed in 10% buffered formalin and embedded in paraffin. Five-micrometer thick sections were stained with hematoxylin and eosin. The Bielshowesky's silver impregnation was used to evaluate axonal population (Luna 1968).

Immunohistochemistry

Paraffin sections were exposed to monoclonal antibody raised against mouse non-phosphorylated neurofilament H (Trapp *et al*. 1998). Sections were de-paraffinized, blocked with 3% normal goat serum, incubated with SMI-32 (1 : 1000) (room temperature, 30 min) washed and incubated with goat anti-mouse IgG (room temperature, 30 min), and ColonoPAP (30 min). SMI-32-positive axons were visualized with 3,3′-diaminobenzidine.

Microscopes

All slides of histopathology and immunocytochemistry were analyzed under an Olympus BX52TF microscope (Olympus, Tokyo, Japan). A DP50-CU microscope digital camera system (Olympus) was used for all photographs. ViewfinderLite™ software (Olympus), with the digital camera attached to the microscopes, was used to acquire images. StudioLite™ software (Olympus) was used to edit and analyze images recorded.

Image analysis technique

Image Pro Plus software (MediaCybernetics, USA) was used to quantify areas stained by Bielshowesky's silver staining, and immunohistochemistry (with anti-SMI-32). Spinal cords of six animals taken from each experimental group were used for the analysis. The spinal cord sections were photographed in a series of six frames (a total of 36 pictures for each group), and assessed by two examiners, double-blind assessment.

T cell proliferation assay

The proliferation response of spleen cells was tested 14 days after the first MOG injection. Four animals of each group were killed by cervical dislocation, the spleens removed and placed in RPMI 1640 medium supplemented with 2 mM glutamine, 50 μM 2-mercaptoethanol, antibiotics (100 U/mL penicillin G, 100 μg/mL streptomycin) and 10% heat-inactivated fetal calf serum (all from Beit Haemek, Israel). Splenocytes were then plated at a concentration of 3×10^5 cells/well. Peptides were added as follows: MOG (2 and 10 μg/well), purified protein derivative from *Mycobacterium tuberculosis* (PPD), and concanavalin A (Con A) (2 μg/well) in triplicate wells. The cells were incubated for 72 h at 37°C in humidified air containing 5% CO_2. [^{3}H]Thymidine (1 μCi/well) was added for the last 16 h of incubation and the cultures were then harvested and counted using a Matrix 96 Direct beta counter (Packard Instr., Meridien, CT, USA). The proliferative response was measured using [^{3}H]thymidine incorporation expressed as mean counts per minute (CPM) of triplicate wells.

Zymography

Frozen brain segments were homogenized in 50 mM Tris-HCl, 0.2 M NaCl, 5 mM $CaCl_2$, 0.02% Brij 35 (w/v), pH 7.6 and centrifuged at 10 000 × *g*, 5 min, 4°C. Equal amounts of protein (Bradford) were separated on gelatin-impregnated (1 mg/mL) 8% sodium dodecyl sulfate–polyacrylamide gel electrophoresis under non-reducing conditions and stained with 0.5% Coomassie G 250 in methanol/acetic acid/H_2O (30 : 10 : 60). Bands intensity (total MMP enzymatic activity) determined by densitometry (Image Gauge V3) is presented as (%) of control. In HT-1080 cells, MMP-2− 9 activation determined in sample media collected 6 and 24 h after serum removal and assayed as above.

Statistical analysis

The statistical significance of differences in the clinical severity of EAE following MOG-induction between the MOG and AD4-treated mice groups was evaluated using Student's *t*-test.

Results

Crossing the blood–brain barrier

AD4 (10–30 mg/kg) was injected intraperitoneally or administered orally (160 mg/kg) to mice. Fifteen min later, the animals were perfused with 100 mL of cold saline to wash out circulating AD4 from the brain. The brains were rapidly removed and extracted with methanol. The brain extracts were divided into two parts, one was reacted with 3,7-dimethyl-4-bromomethyl-6-methyl-1,2-diazobicyclo-octa-3,6-diene-2,8-dione (monobromobimane), a fluorescent thiol-selective tag and applied directly onto high performance liquid chromatography (HPLC) reverse-phase (C18) column and the other was treated with 0.3 mM *N*-ethylmaleimide (NEM) to block SH groups prior to monobromobimane tagging and then applied to HPLC. AD4 was identified in the brain as a new fluorescent peak migrating at the retention time of AD4 standard (results are taken from orally administered AD4). It was absent in control brain samples and protected by NEM pretreatment (Fig. 1a). Other thiols present in the brain, e.g. GSH, cysteine, were separated by HPLC as tagged-fluorescent thiols and identified by tagged-standards run by HPLC under the same running conditions (Fig. 1a, lower panel). In contrast, *N*-acetylcysteine (10–30 mg/kg) that was injected intraperitoneally or administered orally (160 mg/kg) did not appear in the brain extracts indicating no entry into the brain (results are taken from orally administered NAC) (Fig. 1b). It should be pointed out that an increase in cysteine level indicates NAC penetration (Fig. 1b). However no elevation in NAC itself suggest a lower efficiency and a fast decomposition that was not observed with AD4. A more detailed pharmacokinetic study should clarify the features of these thiols in the brain. Endogenous GSH and cysteine similar to AD4 were absent in NEM-treated samples. The advantage of the fluorescent assay relies on selective tagging of thiol groups and verification of the obtained peaks by selectively blocking the thiol group with NEM.

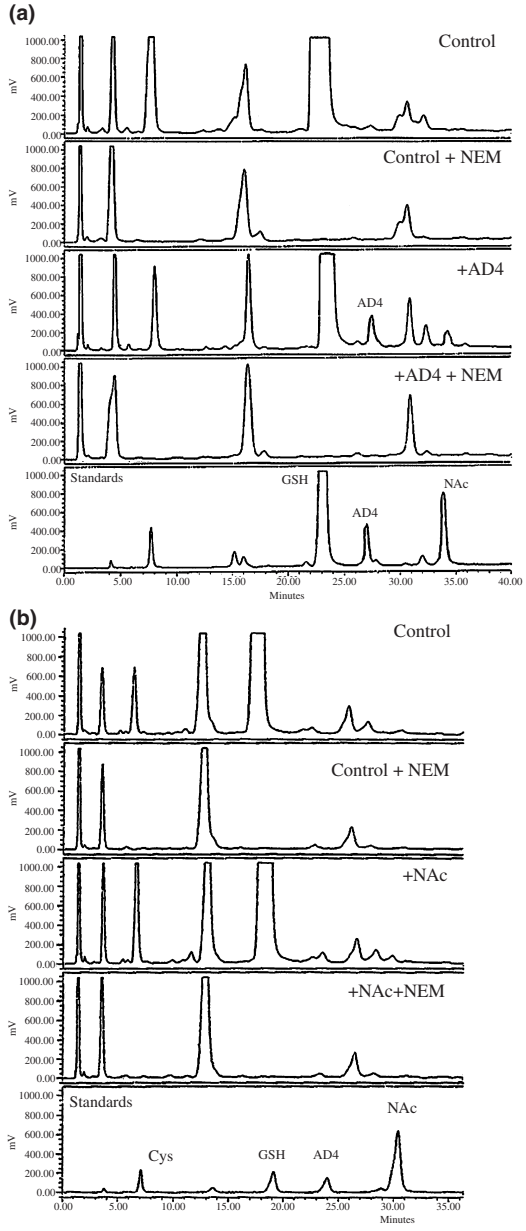

Fig. 1 AD4 crosses the blood–brain barrier determined by HPLC. (a) AD4 and (b) *N*-acetylcysteine (NAC) were administered orally (160 mg/kg). Brain extracts were divided into two parts, one was reacted with 3,7-dimethyl-4-bromomethyl-6-methyl-1,2-diazobicyclo-octa-3,6-diene-2,8-dione (monobromobimane), and the other was reacted first with 0.3 mM *N*-ethylmaleimide (NEM) and then with monobromobiman. AD4 was identified as a new fluorescent peak (absent in control brain samples). The endogenous thiols GSH and cysteine were identified according to the retention time of standards tagged with monobromobimane and similar to AD4 were absent in NEM-treated samples. NAC was absent from the chromatogram showing no crossing into the brain.

Copper-chelating properties of AD4

Copper chelation by the thiol group of AD4 was determined in a cell-free system. Hydroxyl free radicals (·OH) generated by ascorbic acid and copper ions (20 μM) were visualized as HTA fluorescence (see Methods; Fig. 2). The fluorescence signal induced by 20 μM Cu^{2+} was eliminated with 40 μM AD4, demonstrating a 2 : 1 ratio of AD4/Cu^{2+} (Fig. 2). *N*-Acetylcysteine (NAC) and GSH displayed similar chelating activity (data not shown).

Cell membrane permeation and thiol reloading

The efficacy of AD4 and NAC at protecting cells from oxidative stress was examined in red blood cells. Human red blood cells (RBC) were depleted of endogenous thiols by a

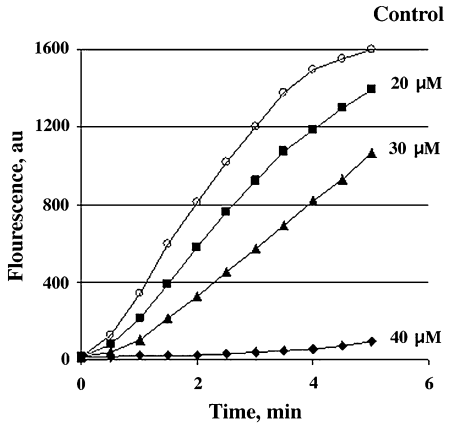

Fig. 2 Copper chelating properties of AD4. Copper ions catalyze ·OH radical formation in the presence of ascorbic acid and air oxygen. Terphthalic acid (TA) traps ·OH radicals and is converted to the fluorescence hydroxyterphthalic acid (HTA). The appearance of HTA fluorescence was monitored at 425 nm (ex 315 nm) in the presence of increasing concentrations of AD4, as indicated. AD4 appeared to form a stoichiometric [Cu–AD4] complex, preventing the redox cycling of Cu^{+}/Cu^{2+}.

ROS-generating compound, tert-butyl-hydroxyperoxide (t-BHP; 0.5 mM). After extensive washings, the GSH-depleted RBC were incubated with increasing concentrations of AD4 or NAC as indicated, and their thiol content was determined using 5,5′-dithiobis(2-nitrobenzoic acid) (DTNB; Fig. 3a,b). AD4 at 1.0 mM restored the RBC thiol pool to the initial value (Fig. 3b) whereas 1.0 mM NAC displayed a considerably smaller effect (Fig. 3a). Thiol content was increased to ∼220% at higher AD4 concentration (5 mM) while NAC at this concentration increased thiol level to 62%. These results indicate that AD4 is approximately threefold more efficient then NAC at restoring intracellular thiol pools, probably due to the better penetration into the cell.

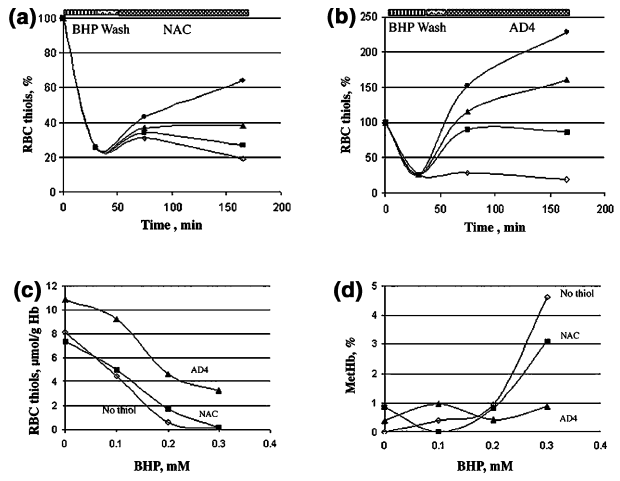

Fig. 3 AD4 protects intracellular proteins from oxidation. Freshly obtained human red blood cells (hRBC) were depleted of endogenous thiols by the addition of tert-butyl hydroxyperoxide (t-BHP) were supplemented by NAC (a) and AD4 (b) at the indicated concentrations. Non-protein thiol content was determined using the specific thiol reagent dithio-5-nitro-benzoate (DTNB) at 412 nm. (c) Thiol level reduction with increasing t-BHP in NAC, AD4 and in non-treated cells was monitored by DTNB (see b). (d) The rate of hemoglobin (Hb) oxidation (Met-Hb) at increasing t-BHP concentrations was followed at absorbance at 630 nm measured before and after the addition of KCN.

Next we determined the correlation of thiol levels and protection from protein oxidation inside the cells. Oxidation of hemoglobin (Hb) to oxyhemoglobin (metHb) in RBC was correlated with tBHQ a reagent that generates free radicals (Fig. 3c). RBC pre loaded with either AD4 (5 mM) or NAC (5 mM) were incubated with tBHP that caused progressive loss of intracellular thiols and an increase in oxygenated hemoglobin (Fig. 3c). In AD4-treated cells thiol levels increased in spite of tBHQ and showed normal levels of metHb (Fig, 3c,d). In contrast, in control- and NAC-treated cells a steep increase in metHb was apparent consistent with a lower thiol content (Fig. 3c,d). Unlike NAC, AD4 appeared to integrate into the redox machinery of human RBC and effectively protect Hb from oxidation.

Depletion of GSH by buthionine sulfoximine (BSO), an inhibitor of gamma-glutamyl-cysteine-synthetase the rate-limiting enzyme in GSH synthesis, causes cell death both *in vivo* and in tissue culture (Miller and Henderson 1986). When applied to SH-5H5Y cells BSO (0.125–0.5 mM) caused cell death that was completely prevented by AD4 (1 mM) (data not shown). As depleted GSH cannot be re-synthesized in the presence of BSO, AD4 seemed to take over the role of GSH, acting as an SH donor.

AD4 protects against cisplatin (CDDP) induced ROS production and inhibits phosphorylation of JNK and p38 MAPKs

To test whether the ROS activated MAPK signaling pathway (Johnson and Lapadat 2002) is the site of action of AD4 we used the anti-tumor drug cisplatin (CDDP), previously shown to increase intracellular ROS and induce apoptosis via activating the MAPK pathway in transformed rat embryo fibroblasts DHER14 cells (Benhar *et al*. 2001).

Scavenging of free radicals was tested by dichlorofluorescein diacetate bis(acetoxymethyl) (DCF-DA) assay. DCF-DA is hydrolyzed to 2′,7′-dichlorofluorescein diacetate upon entering the cell and emits strong fluorescent signal (538 nm) by reacting with ROS. Pre-incubation of DHER14 cells with AD4 or NAC (1 mM) suppressed CDDP (100 μM)-induced ROS accumulation during 8 h, measured at 2 h intervals (Fig. 4a). Interestingly, AD4 reduced ROS below basal level indicative of ROS production and accumulation under normal cell culture conditions even in the absence of an exogenous insult.

ROS induced (CDDP; 100 μM) phosphorylation of MAPKs, p38 and JNK was tested by immunoblotting

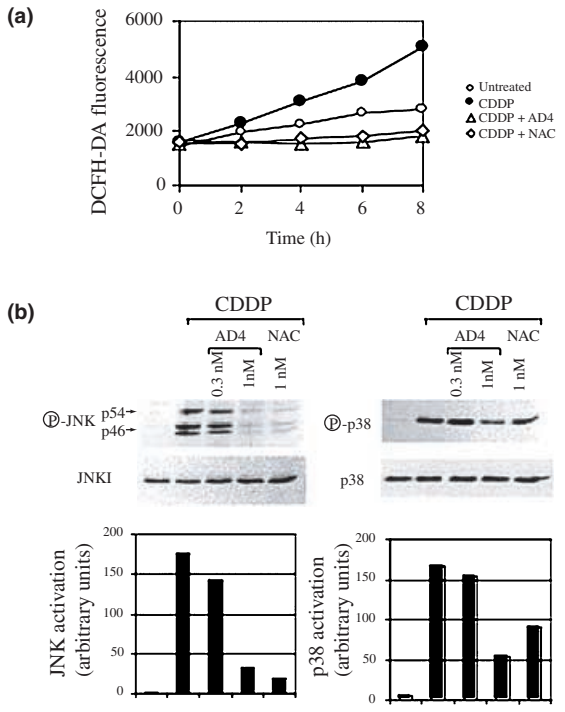

Fig. 4 AD4 scavenges CDDP-induced ROS production and inhibits stress-kinase activation in DHER14 cells. DHER14 cells were treated with antioxidants for 1 h, followed by CDDP. (a) Intracellular ROS was measured with the fluorometric DCF-assay using dichlorofluorescein diacetate bis(acetoxymethyl) (DCF-DA) (see Fig. 1). (b) Cells were lysed and subjected to western blot analysis, using anti-phospho-JNK or anti-phospho-p38 specific antibodies. Parallel blots were reacted with anti-JNK1 or anti-p38 antibodies. Anti-phospho-JNK antibodies recognize the phosphorylated form of the p46 (JNK1) and p54 (JNK2) isoforms. Graphs show (%) activation as quantified by densitometry of immunoblots. Results are representative of three independent experiments.

with antibodies selective for the phosphorylated form of the two enzymes (Fig. 4b). The significant increase in p38 and JNK phosphorylation was reduced by AD4. AD4 displayed a significant higher efficiency at inhibiting p38 phosphorylation compared with NAC (Fig. 4b). The overall level of the two enzymes was not changed as demonstrated with antibodies selective to the non-phosphorylated enzymes.

AD4 improves motor function and suppresses MOG-induced chronic EAE mice

The overall combination of reducing properties, Cu^{2+} chelation, BBB permeation, interference with the stress signaling pathway and no apparent toxicity up to 2.0 g/kg body weight (data not shown) led us to investigate the efficacy of AD4 in chronic EAE, the commonly used animal model of MS. EAE is considered a good model to study the acute disseminating encephalomyelitis because it has many clinical and histopathological similarities to the human MS (Bernard *et al*. 1976; Raine 1984). Initial *in vivo* experiments were performed to test the efficacy of AD4 to suppress EAE when given orally in varying doses (5–50 mg/kg) twice daily. (Fig. 5a,b). All mice that received only saline developed clinical signs while AD4-treated mice showed a marked delay in the onset and a significant reduction the severity of the clinical EAE signs.

We then explored AD4 efficiency after the appearance of clinical signs. MOG-injected mice were randomly assigned to one of four groups: (i) control (daily injection of saline); (ii) daily injection of AD4 (200 mg) from the first MOG injection; (iii) daily injection of AD4 (200 mg) from day 8 after first MOG injection; and (iv) daily injection of AD4 (200 mg) from day 14 when first symptoms appears. We found that AD4 was highly effective at suppressing EAE score when administered from day 1 or day 8 after the first MOG injection (Fig. 5a). Notably, even when administered after the appearance of symptoms, a marked improvement in the EAE score was observed (Fig. 5a). Moreover, half of the AD4-treated mice, either by day 1 or 8, remained disease-free while all the MOG-immunized animals developed clinical signs (Fig. 5b). Comparison of sum scores between the subgroups (area under the curve) indicated that all the mice that were treated with AD4, either from day 1, 8 or 14 demonstrated significant improvement (19.55 ± 8.95, $p < 0.0004$, 17.1 ± 11.03, $p < 0.0017$ and 45.7 ± 2.345, $p < 0.0005$, respectively) as compared to the mice treated with MOG alone (78 ± 7.86).

AD4 was effective in reducing disease incident, mean clinical score and disease onset in a dose-dependent manner (Fig. 5c,d). Statistically significant improvement in clinical scores could be demonstrated already at doses of 10 mg/kg 0.9 ± 0.3 versus 2 ± 0.35 in MOG only, $p < 0.05$ Fig. 5(c).

AD4 reduces MOG induced inflammation and axonal damage in mice spinal cord

Histological analysis of spinal cords by hematoxylin and eosin staining 30 days after MOG immunization revealed in the white matter a marked multifocal lymphohistiocytic inflammation both perivascular and diffuse. In contrast, spinal cords sections of MOG + AD4-treated mice showed no signs of inflammation (Fig. 6a). Quantitative assessment of cell number indicated that AD4 treatment reduced lymphocytes infiltration by 78% (0.0026 versus 0.012, $p < 0.001$; Fig. 6b).

Axonal population of longitudinal spinal cord sections from mice with MOG-induced EAE mice were evaluated by Bielshowesky's silver staining. An extended massive damage was apparent in spinal cord of MOG-induced EAE (Fig. 6c) while a complete protection by AD4 was manifested by the absence of inflammatory cells in sections taken from MOG + AD4-treated animals (Fig. 6d). Quantitation of stained sections of naive, MOG-immunized and

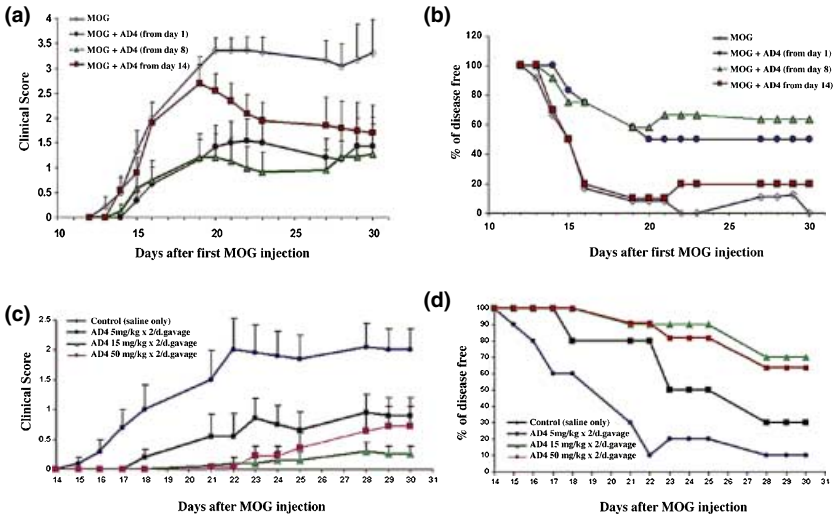

Fig. 5 AD4 suppresses clinical EAE clinical score and improves motor function. Four groups of C3H.SW mice were injected with pMOG 35–55 in CFA supplemented with *Mycobacterium tuberculosis* (Mt) twice (day 1 and 8) and divided into eight groups. (a) The disease course and (b) the percentage of disease-free animals of a representative experiment in which AD4 was administered orally ($n = 4$). (c,d) A representative experiment of four groups: The first group ($n = 12$) injected with saline and the other three groups were treated with AD4200 mg/kg × 2/day (i.p.) as follows: from day 1 ($n = 12$); from day 8 ($n = 11$) or from day 14 (disease onset, $n = 10$). (c) The disease score of a representative experiment; mean daily clinical score ± SEM is shown for each group of mice. (d) Percentage of disease-free animals.

MOG + AD4-treated animals demonstrated reduced axonal damage in AD4-treated mice by 43% (0.38 versus 0.67, $p < 0.001$; Fig. 6d). Furthermore, immunohistochemical analysis with antibodies to SMI-32 confirmed a far-reaching protection from axonal damage (97%) (0.0008 versus 0.03 (arbitrary units) $p < 0.001$ in AD4-treated mice.

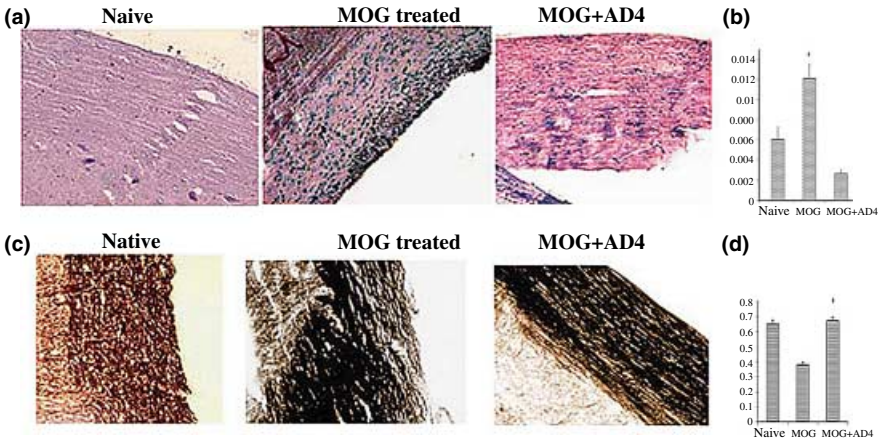

Fig. 6 AD4 suppressed inflammatory infiltrate in longitudinal spinal cord sections, reduces axonal damage in MOG-immunized mice. (a) The histological examination of spinal cords removed from mice 30 days after immunization with MOG. Hematoxylin and eosin staining examined inflammatory effect in longitudinal spinal cords sections. Suppression of inflammatory infiltration was observed in sections of animals treated with MOG together with AD4. (b) Quantification of the results using Image Pro analysis showed the strong AD4 anti-inflammatory effect (MOG versus Naive, $*p < 0.001$; and MOG + AD4 versus MOG, $**p < 0.001$). Arbitrary units represent pixel area of stained lymphocytes. Original magnification of all pictures × 100 showed the strong AD4 anti-inflammatory effect ($*p < 0.001$ in MOG versus naive, and $**p < 0.001$ for MOG + AD4 versus MOG. (c) Histological examination of spinal cords removed from mice 30 days after immunization with MOG. Axonal damage was visualized by Bielshowesky's silver staining of axonal population of longitudinal spinal cord sections of naive, MOG-and MOG + AD4-treated mice. Silver stained sections revealed axonal loss in MOG-treated animals and practically none in MOG immunized mice treated with AD4. (d) Quantification of the stained areas by Image Pro analysis showed MOG versus Naïve $*p < 0.001$ and for MOG + AD4 versus MOG, $**p < 0.001$).

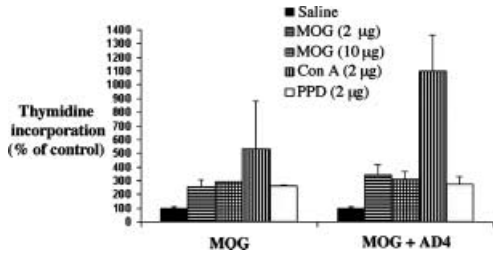

Fig. 7 AD4 treatment following MOG immunization does not alter specific immune response. Splenocytes isolated from MOG-immunized mice treated for 14 days with AD4 (250 mg/kg × 2) or saline were examined for their response to MOG (2 and 10 μg/well), PPD (2 μg/well) and the non-specific antigen Con A (2 μg/well). Activation and proliferative response was measured by [^{3}H]thymidine incorporation (see Methods). Each column represents cpm ± SEM of nine wells (three mice/triplicate).

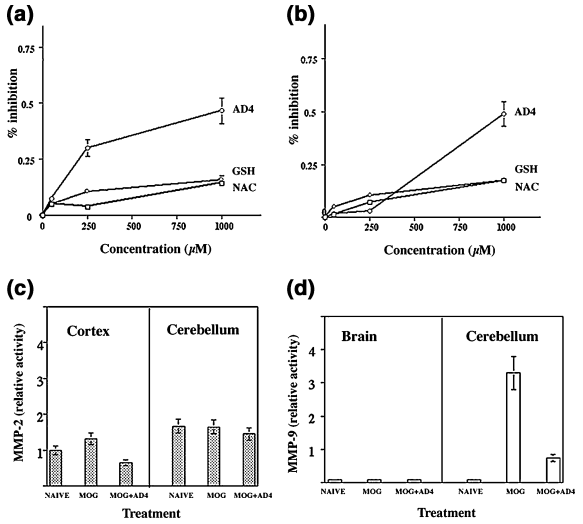

Fig. 8 AD4 inhibits MMP-2 and MMP-9 activation in MOG-treated mice. Secretion of MMP 9 in HT-1080 human fibrosarcoma cells, in the absence of serum was measured after 6 (a) and 24 h (b). The effect of AD4, glutathione (GSH) and NAC at increasing concentrations, as indicated, on MMP-9 activity was determined by zymography. AD4 appeared more potent at inhibiting MMP-9 with potency increasing from 6- to 24-h incubation. MMP-2 (c) and MMP-9 (d) activity over a period of 30 days in naive, MOG injected and MOG + AD4 (200 mg/kg) treated mice of a representative experiments shown in Fig. 3. At day 30 the animals were killed and their cortex and cerebellum removed. MMP-2 and MMP-9 activity were determined by zymography and presented as percent ($n = 4$; carried separately at the two sides of the cortex and cerebellum).

AD4 does not modify the immune response in MOG-immunized mice

We compared the splenocytes-derived T cell response in MOG-immunized mice treated with saline or AD4 to rule out the possibility that the observed differences in clinical and histological manifestations of the disease were due to a generalized immune effect. MOG 35–55-immunized mice were treated for 14 days (three in each group) with AD4 (250 mg/kg × 2) or saline and their recall T-cell proliferative response against MOG, PPD and Con A was assessed. As shown in Fig. 7, the *in vitro* primary proliferative response of both saline and AD4-treated mice against these antigens was comparable. For example exposure to MOG (10 μg/well) increased thymidine incorporation by 294% in saline-treated mice as compared with 312% in the AD4-treated mice (2467 versus 1082 cpm at baseline, respectively). This suggests that AD4 treatment did not affect the proliferative capacity of the periphery lymphoid tissues.

AD4 inhibits metalloproteinase activation in cells and *in vivo*

Susceptible to the redox state of the cell, MMPs play an important role in the invasion of brain parenchyma as immune cells, and through BBB breakdown and demyelination. To test whether MMP production was inhibited by AD4 we studied HT-1080 fibrosarcoma cells, known to secrete MMP-2 and MMP-9 into the media. The level of enzymes produced at 6 and 24 h was reduced by AD4, GSH and NAC in a dose-response manner as determined by zymography (Fig. 8a,b). AD4 efficacy at inhibiting MMP-9 increased after 24-h incubation in contrast to GSH and NAC. Such a prolonged action suggests a slow degradation of AD4 perhaps as a result of efficient penetration into the cell protecting from oxidation (see Fig. 3). GSH and NAC were more potent than AD4 at inhibiting MMP-2 activation during 6-h incubation while at 24 h, AD4 potency rose unlike GSH and NAC (data not shown). The enzymatic activity of the recombinant MMPs, however, was not inhibited by AD4 (data not shown) consistent with AD4 interference upstream to the activated enzyme, maybe via the MAPK signaling pathway.

MMPs activation *in vivo*, in cortex and cerebellum of EAE mice was conducted 30 days after onset of the disease. MMP-2 production was small and no significant changes were detected in cortices of naive, MOG – (average score of 2) and MOG + AD4-treated mice (average score of 0; Fig. 8c). In contrast, MMP-9 activity was drastically increased in the cerebellum of MOG-immunized animals ($n = 4$) consistent with elevated MMP-9 in EAE and MS patients and considerably reduced in MOG + AD4-treated animals ($n = 4$; Fig. 8d).

Discussion

We have characterized a novel thiol antioxidant that crosses the BBB and effectively suppresses clinical and physiological signs of mouse model of MS when injected intraperitoneally or taken orally. As a thiol reagent AD4 forms a stoichiometric complex with Cu^+, presumably by a mechanism earlier described for GSH (Ohta *et al.* 2000), acting to reduce oxygen free radicals. Because Cu^{2+} acts catalytically,

small amounts of AD4 would be effective at preventing OS, scavenging minuscule excess of the free divalent ions formed in the brain under pathological conditions.

The striking features of AD4 at crossing the BBB when given orally and the readiness permeation across the cell membrane are essential for reducing oxidative stress in the brain. The extraordinary incorporation of AD4 into the cellular redox machinery was established in human RBC used as a model of a cell fully equipped with enzymatic systems of GSH synthesis, oxidation, reduction and thiol–disulfide exchange. Preincubation with AD4 showed a remarkable restoration (200%) of intracellular thiols that had been depleted by tBHQ, an ROS-producing agent (Behl *et al*. 1994). In contrast, NAC efficacy was significantly smaller ($\sim$ 60%). The superiority of AD4 results from the membrane permeation of the neutral molecule (AD4) over the charged NAC. Preventing Hb from oxidation was correlated with higher thiol levels, demonstrating active participation of AD4 in the cell redox machinery. At this stage it cannot be determined which portion of the measured thiol pool consists of AD4 that penetrated the cell, or GSH generated from GSSG by AD4. Survival of SH-SY5Y neuroblastoma after BSO treatment is consistent with an effective substitution of depleted GSH by AD4.

The present study shows that in tissue culture, AD4 inhibits the phosphorylation of JNK and p38 most likely as the result of scavenging ROS. *In vivo*, AD4 is predicted to offer a better protection then GSH and NAC because of its membrane crossing capacity. Inhibition of the MAPK signaling pathway indicates attenuation of a vast array of physiological processes downstream of pro-inflammatory gene products, through AP-1, p53, AFT-2 and others. Because the MAPK signaling pathway involves AP-1 activation of inducible MMP genes and TPA responsive elements (TRE) at their proximal promoters, interception of MAPK signaling could restrain MMP transcription and subsequent activity. Consistent with this possibility, we show that AD4 prevents MMP-2 and MMP-9 production in MOG-treated mouse brain. MMP-9 levels were previously shown to be significantly elevated in the serum and CSF of both MS patients and EAE mice, and the use of MMP inhibitors (Gijbels *et al*. 1992; Hewson *et al*. 1995; Liedtke *et al*. 1998) and blocking of AP-1 that regulates MMP's was correlated with improvement of motor function and other clinical signs. Furthermore, interferon-1β currently used in MS therapy, decreases T-lymphocytes migration *in vitro* by inhibiting MMP-9 (Leppert *et al*. 1996; Stuve *et al*. 1996; Yong *et al*. 1998; Uhm *et al*. 1999). Consistent with these experiments, we propose that targeting ROS-activation of MAPK signaling underlines the beneficial effects of AD4 in EAE. Concurrent with MMP inhibition, our results clearly demonstrate a delay in the onset of EAE and a significant suppression of the severity and incidence of the clinical signs such as paralysis and lymphocytes migration. A drastic reduction in the inflammation response and axonal damage at the spinal cords by AD4 indicates inhibition of the inflammation process at the CNS. Furthermore, by lowering MAPK cascade and precluding MMP 9 activation, AD4 could inhibit the transmigration of T-lymphocytes across the subendothelial basement membrane and into the perivascular space and the parenchyma of the brain.

In addition, the *in vitro* specific response of T cells for MOG, PPD and Con A was similar in the AD4-treated and MOG-immunized mice, suggesting that the beneficial effect of AD4 is probably not mediated via interference with immunological mechanisms. ROS scavenging by AD4 might halt the inflammation process at the time when damaged tissues (i.e. neurons and oligodendrocytes) recruit macrophages that release H_2O_2, NO and other free radicals (Hogg 2000). Therefore, effective protection of SH-SY5Y neuroblastoma cells offered by AD4 against NO toxicity could result also from shielding a vital SH-group in a protein involved in the progression of EAE such as MMPs (Hogg 2000; Gu *et al*. 2002). Protecting proteins and/or GSH from nitrosylation by AD4 could represent an additional benefit to prevent OS damage

In conclusion, as demonstrated in this study, AD4 delays and partially reverses disease progression. It inhibits axonal damage, and MMP activation and inflammation in a mouse model of MS. Given its non-toxic features, oral bioavailability, crossing the BBB and inhibition of MAPK signaling-pathway, AD4 could prevent pathogenic consequences of elevated ROS and therefore could be evaluated for its efficacy in treating human MS and other neurodegenerative disorders.

Acknowledgements

This work was supported by funds from Novia Pharmaceuticals and Lili Safra to DA. We thank Y. Aharonowitz for helpful discussions and M. Yanko for HPLC separations.

References

Adler V., Yin Z., Tew K. D. and Ronai Z. (1999) Role of redox potential and reactive oxygen species in stress signaling. *Oncogene* **18**, 6104–6111.

Atlas D., Melamed E. and Offen D. (1999) Brain targeted low molecular weight hydrophobic antioxidant compounds. United States Patent.

Barreto J. C., Smith G. S., Strobel N. H., McQuillin P. A. and Miller T. A. (1995) Terephthalic acid: a dosimeter for the detection of hydroxyl radicals *in vitro*. *Life Sci.* **56**, PL89–96.

Behl C., Davis J. B., Lesley R. and Schubert D. (1994) Hydrogen peroxide mediates amyloid beta protein toxicity. *Cell* **77**, 817–827.

Benhar M., Dalyot I., Engelberg D. and Levitzki A. (2001) Enhanced ROS production in oncogenically transformed cells potentiates c-Jun N-terminal kinase and p38 mitogen-activated protein kinase activation and sensitization to genotoxic stress. *Mol. Cell Biol.* **21**, 6913–6926.

Bernard C. C., Leydon J. and Mackay I. R. (1976) T cell necessity in the pathogenesis of experimental autoimmune encephalomyelitis in mice. *Eur J. Immunol.* **6**, 655–660.

Beutler E. (1974) Red cell metabolism: a manual of Biochemical Methods, pp. 55–59. Grune & Stratton, New York.

Boulton T. G., Nye S. H., Robbins D. J., Ip N. Y., Radziejewska E., Morgenbesser S. D., DePinho R. A., Panayotatos N., Cobb M. H. and Yancopoulos G. D. (1991) ERKs: a family of protein-serine/threonine kinases that are activated and tyrosine phosphorylated in response to insulin and NGF. *Cell* **65**, 663–675.

Butterfield D. A., Koppal T., Subramaniam R. and Yatin S. (1999) Vitamin E as an antioxidant/free radical scavenger against amyloid beta-peptide-induced oxidative stress in neocortical synaptosomal membranes and hippocampal neurons in culture: insights into Alzheimer's disease. *Rev. Neurosci.* **10**, 141–149.

Cherny R. A., Atwood C. S., Xilinas M. E. *et al.* (2001) Treatment with a copper-zinc chelator markedly and rapidly inhibits beta-amyloid accumulation in Alzheimer's disease transgenic mice. *Neuron* **30**, 665–676.

Cuzner M. L., Gveric D., Strand C., Loughlin A. J., Paemen L., Opdenakker G. and Newcombe J. (1996) The expression of tissue-type plasminogen activator, matrix metalloproteases and endogenous inhibitors in the central nervous system in multiple sclerosis: comparison of stages in lesion evolution. *J. Neuropathol. Exp. Neurol.* **55**, 1194–1204.

Davis R. J. (1993) The mitogen-activated protein kinase signal transduction pathway. *J. Biol. Chem.* **268**, 14553–14556.

Emerson M. R. and LeVine S. M. (2000) Heme oxygenase-1 and NADPH cytochrome P450 reductase expression in experimental allergic encephalomyelitis: an expanded view of the stress response. *J. Neurochem.* **75**, 2555–2562.

Finkel T. and Holbrook N. J. (2000) Oxidants, oxidative stress and the biology of ageing. *Nature* **408**, 239–247.

Gijbels K., Masure S., Carton H. and Opdenakker G. (1992) Gelatinase in the cerebrospinal fluid of patients with multiple sclerosis and other inflammatory neurological disorders. *J. Neuroimmunol.* **41**, 29–34.

Gilgun-Sherki Y., Melamed E. and Offen D. (2001) Oxidative stress induced-neurodegenerative diseases: the need for antioxidants that penetrate the blood brain barrier. *Neuropharmacology* **40**, 959–975.

Gilgun-Sherki Y., Rosenbaum Z., Melamed E. and Offen D. (2002) Antioxidant therapy in acute central nervous system injury: current state. *Pharmacol. Rev.* **54**, 271–284.

Grinberg L. N., Rachmilewitz E. A. and Newmark H. (1994) Protective effects of rutin against hemoglobin oxidation. *Biochem. Pharmacol.* **48**, 643–649.

Gu Z., Kaul M., Yan B., Kridel S. J., Cui J., Strongin A., Smith J. W., Liddington R. C. and Lipton S. A. (2002) S-Nitrosylation of matrix metalloproteinases: signaling pathway to neuronal cell death. *Science* **297**, 1186–1190.

Hewson A. K., Smith T., Leonard J. P. and Cuzner M. L. (1995) Suppression of experimental allergic encephalomyelitis in the Lewis rat by the matrix metalloproteinase inhibitor Ro31–9790. *Inflamm. Res.* **44**, 345–349.

Hogg N. (2000) Biological chemistry and clinical potential of *S*-nitrosothiols. *Free Radic. Biol. Med.* **28**, 1478–1486.

Johnson G. L. and Lapadat R. (2002) Mitogen-activated protein kinase pathways mediated by ERK, JNK, and p38 protein kinases. *Science* **298**, 1911–1912.

Lehmann D., Karussis D., Misrachi-Koll R., Shezen E., Ovadia H. and Abramsky O. (1994) Oral administration of the oxidant-scavenger *N*-acetyl-L-cysteine inhibits acute experimental autoimmune encephalomyelitis. *J. Neuroimmunol.* **50**, 35–42.

Leppert D., Waubant E., Burk M. R., Oksenberg J. R. and Hauser S. L. (1996) Interferon beta-1b inhibits gelatinase secretion and *in vitro* migration of human T cells: a possible mechanism for treatment efficacy in multiple sclerosis. *Ann. Neurol.* **40**, 846–852.

Liedtke W., Cannella B., Mazzaccaro R. J., Clements J. M., Miller K. M., Wucherpfennig K. W., Gearing A. J. and Raine C. S. (1998) Effective treatment of models of multiple sclerosis by matrix metalloproteinase inhibitors. *Ann. Neurol.* **44**, 35–46.

Lindberg R. L., De Groot C. J., Montagne L., Freitag P., van der Valk P., Kappos L. and Leppert D. (2001) The expression profile of matrix metalloproteinases (MMPs) and their inhibitors (TIMPs) in lesions and normal appearing white matter of multiple sclerosis. *Brain* **124**, 1743–1753.

Liu Y., Zhu B., Luo L., Li P., Paty D. W. and Cynader M. S. (2001) Heme oxygenase-1 plays an important protective role in experimental autoimmune encephalomyelitis. *Neuroreport* **12**, 1841–1845.

Luna L. G. (1968) *Manual of Histologic Staining Methods of Armed Forces*, pp. 193–194. McGraw-Hill.

Marracci G. H., Jones R. E., McKeon G. P. and Bourdette D. N. (2002) Alpha lipoic acid inhibits T cell migration into the spinal cord and suppresses and treats experimental autoimmune encephalomyelitis. *J. Neuroimmunol.* **131**, 104–114.

Mehindate K., Sahlas D. J., Frankel D., Mawal Y., Liberman A., Corcos J., Dion S. and Schipper H. M. (2001) Proinflammatory cytokines promote glial heme oxygenase-1 expression and mitochondrial iron deposition: implications for multiple sclerosis. *J. Neurochem.* **77**, 1386–1395.

Mendel I., Katz A., Kozak N., Ben-Nun A. and Revel M. (1998) Interleukin-6 functions in autoimmune encephalomyelitis: a study in gene-targeted mice. *Eur. J. Immunol.* **28**, 1727–1737.

Miller A. C. and Henderson B. W. (1986) Effect of DL-buthionine-S,R.-sulfoximine on the growth of EMT6 and RIF mouse tumors. *J. Natl Cancer Inst.* **77**, 505–510.

Ohta Y., Shiraishi N., Nishikawa T. and Nishikimi M. (2000) Copper-catalyzed autoxidations of GSH and 1-ascorbic acid: mutual inhibition of the respective oxidations by their coexistence. *Biochim. Biophys. Acta* **1474**, 378–382.

Opazo C., Huang X., Cherny R. A. *et al.* (2002) Metalloenzyme-like activity of Alzheimer's disease beta-amyloid. Cu-dependent catalytic conversion of dopamine, cholesterol, and biological reducing agents to neurotoxic H(2)O(2). *J. Biol. Chem.* **277**, 40302–40308.

Raine C. S. (1984) Biology of disease: analysis of autoimmune demyelination: its impact upon multiple sclerosis. *Lab. Invest.* **50**, 608–635.

Rothstein J. D. (1996) Therapeutic horizons for amyotrophic lateral sclerosis. *Curr. Opin. Neurobiol.* **6**, 679–687.

Sen C. K. (1998) Redox signaling and the emerging therapeutic potential of thiol antioxidants. *Biochem. Pharmacol.* **55**, 1747–1758.

Stuve O., Dooley N. P., Uhm J. H., Antel J. P., Francis G. S., Williams G. and Yong V. W. (1996) Interferon beta-1b decreases the migration of T lymphocytes *in vitro*: effects on matrix metalloproteinase-9. *Ann. Neurol.* **40**, 853–863.

Takahashi E. and Berk B. C. (1998) MAP kinases and vascular smooth muscle function. *Acta Physiol. Scand.* **164**, 611–621.

Trapp B. D., Peterson J., Ransohoff R. M., Rudick R., Mork S. and Bo L. (1998) Axonal transection in the lesions of multiple sclerosis. *N. Engl. J. Med.* **338**, 278–285.

Uhm J. H., Dooley N. P., Stuve O., Francis G. S., Duquette P., Antel J. P. and Yong V. W. (1999) Migratory behavior of lymphocytes isolated from multiple sclerosis patients: effects of interferon beta-1b therapy. *Ann. Neurol.* **46**, 319–324.

Whitham R. H., Bourdette D. N., Hashim G. A., Herndon R. M., Ilg R. C., Vandenbark A. A. and Offner H. (1991) Lymphocytes from SJL/J mice immunized with spinal cord respond selectively to a peptide of proteolipid protein and transfer relapsing demyelinating experimental autoimmune encephalomyelitis. *J. Immunol.* **146**, 101–107.

Yong V. W., Chabot S., Stuve O. and Williams G. (1998) Interferon beta in the treatment of multiple sclerosis: mechanisms of action. *Neurology* **51**, 682–689.

Yong V. W., Power C., Forsyth P. and Edwards D. R. (2001) Metalloproteinases in biology and pathology of the nervous system. *Nat. Rev. Neurosci.* **2**, 502–511.

Zor T. and Selinger Z. (1996) Linearization of the Bradford protein assay increases its sensitivity: theoretical and experimental studies. *Anal. Biochem.* **236**, 302–308.